SUPPLEMENTAL MATERIAL

Supplemental Methods

Generation of patient-derived iPSC lines

Peripheral blood mononuclear cells (PBMCs) from the patient with DMD and his healthy brother were reprogrammed to iPSCs at the UT Southwestern Wellstone Myoediting Core as previously described[14].

iPSC maintenance and differentiation

iPSC culture and differentiation were performed as previously described[20]. Briefly, iPSCs were cultured on Matrigel-coated tissue culture polystyrene plates and maintained in Essential 8 media (Thermo Fisher). iPSCs were passaged at 70-80% confluency using Versene (Thermo Fisher). Cardiac differentiation of iPSCs was induced when iPSCs achieved confluency by treating cells with CHIR99021 (Selleckchem) in RPMI (Thermo Fisher) supplemented with B27 without insulin (Thermo Fisher) for 24 hr (from day (d) 0 to d1). The medium was replaced with RPMI/B27-insulin at d1. The cells were then treated with IWP4 (Stemgent) in RPMI/B27-insulin at d3 and the medium was refreshed at d5 with RPMI/B27-insulin. iPSC-derived cardiac myocytes (iPSC-CMs) were maintained in basal medium containing RPMI supplemented with B27 (Thermo Fisher) starting from d7, with the medium changed every 3-4 days. Ascorbic acid at 50 µg/ml was added to both media. Metabolic selection of cardiac myocytes was performed for 6 days starting d10 post-differentiation by culturing cells in RPMI without glucose (Thermo

Fisher) supplemented with 5 mM sodium DL-lactate and CDM3 supplement[21]. iPSC-CMs were replated at $1x10^6$ cells per well of a 6-well plate at d11 post-differentiation using Tryple Express (Thermo Fisher). On d16, medium was changed to basal medium. On d20, medium was changed to basal medium containing 100nM T3, 1 μM dexamethasone and 100ng/ml Long R3 IGF-1 (all Sigma-Aldrich). iPSC-CMs cultured in this medium have previously been shown to attain structural and functional maturity similar to neonatal cardiomyocytes[22, 23]. Starting on d30, iPSC-CMs were cultured in basal medium.

Generation of corrected DMD iPSC lines

DMD iPSC lines corrected by reframing (+1nt insertion; Online Figure I) or exon skipping were generated by nucleofection of the DMD iPSC line as previously described[14]. A single-cell suspension of $1x10^6$ iPSCs was mixed with 5 μg of PX458-sgRNA-2A-GFP plasmid containing our previously published guide RNA[14] and nucleofected using the P3 Primary Cell 4D-Nucleofector X Kit (Lonza) according to the manufacturer's protocol. Three days after nucleofection, iPSCs expressing GFP were isolated by fluorescence-activated cell sorting (FACS) and cultured further. Single GFP^+ iPSC clones were picked, expanded and sequenced. Corrected lines were maintained and differentiated as stated above. The sequence of the gRNA used in this study was as follows: 5'-ATCTTACAGGAACTCCAGGA-3'. This gRNA targets the 5′ boundary of exon 45 of the *DMD* gene[14].

Morphological and structural assessments

For cell size measurements, d35 iPSC-CMs were incubated with Alexa Fluor 555-conjugated wheat germ agglutinin (WGA, W32464; Thermo Fisher) diluted 1:500 in Ca^{2+}- and Mg^{2+}-free PBS for 15 minutes, and then fixed and stained for sarcomeric α-actinin as described below. Cell size was quantified using Fiji software.

Sarcomere length measurements were performed as previously described[24, 25]. D35 iPSC-CMs were treated with WGA as described above, fixed and stained for sarcomeric α-actinin as described below. Sarcomere lengths were quantified by plotting a line intensity profile in Fiji software over the longitudinal axis of cells as previously described[24].

Immunofluorescence staining

For immunofluorescence staining, cells were replated on glass surfaces, except for experiments in Fig. 4E and F, wherein cells were replated on PDMS 527 surfaces. For immunofluorescence staining of dystrophin, cells were fixed with ice-cold acetone for 10 minutes at -20°C. Otherwise, cells were fixed with 4% paraformaldehyde for 10 min. In both cases, cells were blocked with 5% goat serum/0.1% Tween-20 (Sigma-Aldrich) for 1 hr. Primary and secondary antibodies were added to cells in blocking buffer for 2 hr and 1 hr, respectively. Nuclei were counterstained using DAPI. Antibodies used in this article are: dystrophin (MANDYS8, D8168, Sigma-Aldrich, 1:800 dilution), sarcomeric α-actinin (clone EA-53, A7811, Sigma-Aldrich, 1:600 dilution), RYR2 (HPA020028, Sigma Aldrich, 1:200 dilution), cardiac troponin I (47003, Abcam, 1:600 dilution). The following Alexa Fluor-conjugated isotype-specific secondary antibodies (Thermo Fisher, 1:600 dilution) were used: Goat anti-rabbit Alexa 488 (A11008), Goat anti-mouse Alexa 488 (A11001),

Goat anti-mouse Alexa 647 (A21235), Goat anti-mouse IgG1 Alexa 488 (A21121), Goat anti-mouse IgG2b Alexa 647 (A21242). In all immunofluorescence experiments, antibody specificity was confirmed by staining iPSC cells, which do not express the proteins we analyzed in this study. iPSC-CMs stained with secondary antibodies only were used as negative controls to distinguish genuine staining from background and to adjust imaging settings.

Western blot

Western blot experiments were performed as previously described[12]. For iPSC-CMs, cells were lyzed in standard RIPA buffer and 12 µg of total protein were loaded onto a 4-20% gel. For mouse hearts, tissues were crushed into fine powder using a liquid nitrogen-frozen crushing apparatus and 50 µg of total protein were loaded onto a 4-20% gel. Gels were run at 80V for 15min and changed to 150V for 90min, followed by transfer to a polyvinylidene difluoride membrane at 100V for 90min at 4°C. The membrane was probed with mouse anti-dystrophin antibody (MANDYS8, D8168, Sigma-Aldrich, 1:1000 dilution) at 4°C overnight or anti-vinculin antibody (V9131, Sigma-Aldrich, 1:1250 dilution) for 1h at room temperature. Goat anti-mouse HRP antibody (#1706516, Bio-Rad Laboratories, 1:1000 dilution) was used as secondary antibody. Blots were developed using Western Blotting Luminol Reagent (Santa Cruz, sc-2048). For Fig. 1D, we used vinculin as a loading control. For Fig. 4D and 5B, we used total protein expression as a loading control[26]. Briefly, we stained blots with 0.01% Ponceau S (Sigma-Aldrich) in 1% acetic acid for 10 mins and washed them with distilled water before imaging. Whole lanes were used as loading control to normalize the expression of dystrophin.

Functional analyses of iPSC-CMs

Calcium handling and contractility were performed on iPSC-CMs at d35 post-differentiation. Cells were plated at single-cell density on flexible polydimethylsiloxane (PDMS) 527 substrates (Young's modulus=5kPa) prepared according to a previously established protocol[27]. For analysis of calcium handling, iPSC-CMs were loaded with the fluorescent calcium indicator Fluo-4 AM (Thermo Fisher) at 2 μM. Spontaneous Ca^{2+} transients of beating iPSC-CMs were imaged at 37°C using a Nikon A1R+ confocal system at 114 frames per second. Ca^{2+} transients were processed using Fiji software, and analyzed using Microsoft Excel and Clampfit 10.7 software (Axon Instrument). The calcium release phase was represented with time to peak, which was calculated as the time from baseline to maximal point of the transient. The calcium reuptake phase was represented with the time constant tau by fitting the decay phase of calcium transients with a first-order exponential function.

For single-cell peak systolic force measurements, videos of contracting iPSC-CMs were captured at 37°C using a Nikon A1R+ confocal system at 59 frames per second in resonance scanning mode. Contractile force generation of single iPSC-CMs was quantified using a previously established method[24]. In brief, movies of single contracting iPSC-CMs were analyzed using Fiji. Maximum and minimum cell lengths during contractions as well as cell widths were measured, and peak systolic forces generated calculated using a previously published customized Matlab code[24, 28]. From the videos, contraction time and relaxation time were further quantified. Calcium and force measurements were performed at d35 post-differentiation.

Membrane potential measurements were performed on iPSC-CMs at d65 post-differentiation (adenoviral delivery at d35 and further culture for 30 days). Cells were replated at high-density on PDMS 527 substrates and loaded with the fluorescent voltage-sensitive dye FluoVolt (Thermo Fisher) at a 1:1000 dilution. Spontaneous membrane potential transients of beating iPSC-CMs were imaged at 37°C using a Nikon A1R+ confocal system at 114 frames per second. Membrane potential transients were extracted using Fiji software.

Isolation of genomic DNA

Genomic DNA of iPSCs was isolated using DirectPCR Cell (Viagen) according to manufacturer's recommendations.

RT-PCR

RNA was extracted from cells using Trizol (Thermo Fisher) and purified using Direct-zol RNA Miniprep Kit (Zymo Research). cDNA was synthesized using iScript cDNA Synthesis Kit (Bio-Rad). Transcript levels were measured and calculated relative to the expression of RPL13A using KAPA SYBR Fast qPCR Master Mix (KAPA) and 7900HT Fast Real-Time PCR machine (Applied Biosystems). qPCR reactions were performed following the manufacturer's protocol. In brief, enzyme activation was performed at 95°C for 3 minutes, followed by 40 cycles consisting of denaturation at 95°C for 3 seconds and annealing/extension at 60°C for 20 seconds. Sequences of primers used in this study are shown in Online Table I.

Membrane tension measurements

For membrane tension measurements, d50 iPSC-CMs were dissociated and replated on glass surfaces. Cells were loaded with the membrane tension probe Flipper-TR[29] (Cytoskeleton) at 1:1000 in iPSC-CMs culture media and imaged on a fluorescent lifetime imaging microscope (FLIM). Blebbistatin (Sigma-Adrich) was added to the culture media at a final concentration of 5μM to stop beating of CMs to eliminate motion artefacts during imaging. Lifetime data were obtained as previously described[30]. Briefly, the microscope system was calibrated using a fluorescein solution with known lifetimes (i.e. 4.26ns at pH 8.5). Lifetime data was acquired based on 8 phase shifts between camera intensifier and light source. The single-Tau channel – i.e. an image in which each pixel has a lifetime value instead of an intensity value - was generated using SlideBook5. Lifetimes were then directly measured using a custom-written Fiji macro by drawing a 5-pixel-wide line over the membrane section of interest in the intensity channel. Regions of interest were then transferred onto the tau-channel and the average lifetimes directly calculated for these regions. A mask was applied to fluorescence lifetime images to reduce extracellular noise.

Bulk RNA-sequencing

RNA of iPSC-CMs was isolated at d50 post-differentiation as described above. RNA integrity number (RIN) was examined on an Agilent 2200 Tapestation using Agilent RNA Screentape (Agilent Technologies, 5067-5576) and all RNA samples used in the study

have RINs above 9.6. Stranded mRNA-Seq libraries were generated using KAPA mRNA HyperPrep Kit (Roche, KK8581) following manufacturer's protocol. Sequencing was performed on an Illumina Nextseq 500 system using the 75bp high output sequencing kit for single-end sequencing. RNA-seq data analysis was performed as previously described, with modifications[31]. Quality control of RNA-Seq data was performed using FastQC Tool (Version 0.11.4). Sequencing reads were aligned to human GRCh38.p13 (hg38) reference genome using HiSAT2 (Version 2.0.4) with default settings and --rna-strandness F[32]. Aligned reads were counted using featurecount (Version 1.6.0) per gene ID[33]. Differential gene expression analysis was performed with the R package edgeR (Version 3.20.5) using the GLM approach[34]. For each comparison, genes with more than 1 CPM (Count Per Million) in at least three samples were considered as expressed and were used for calculating normalization factor. Multiplicity correction was performed by applying the Benjamini-Hochberg method on the p-values to control the false discovery rate as part of the edgeR algorithm. Cutoff values of absolute fold change greater than 2.0 and false discovery rate less than 0.01 were used to define differentially expressed genes. Normalized gene CPM values were used to calculate RPKM (Reads Per Kilobase per Million mapped reads) values, which were then used for heatmap plotting with hierarchical clustering on genes using R package pheatmap. Gene ontology analysis was performed using Metascape[35]. Principal component analysis (PCA) was performed using R package DESeq2[36].

Generation of adenoviruses

Adenoviruses were generated using the Adeno-X Adenoviral System 3 (Takara Bio). The empty PX458-sgRNA-2A-GFP plasmid was used as a template to generate Ad.Cas9 adenovirus coding for Cas9. The PX458-sgRNA-2A-GFP plasmid containing the abovementioned gRNA was used as a template to generate Ad.Cas9/gRNA adenovirus coding for Cas9 and the gRNA. GFP was first removed from the plasmids by digestion with EcoRI and then cloned into the pAdx-CMV vector containing dsRed. Adenoviruses were generated by transfecting linearized recombinant adenoviral plasmids into a mammalian packaging cell line Adeno-X 293. Primary lysates were used to re-infect Adeno-X 293 cells to generate higher-titer viruses. The viral titer was determined in 293T cells using Adeno-X RapidTiter Kit (Clontech). Adenoviruses were stored in 20 ul aliquots at -80°C. In all experiments, AdCas9 was used as a control vector.

FACS analysis

Quantification of relative cell size was performed as previously described[37]. Living iPSC-CMs were dissociated, stained with DAPI and gated for viability and single cells, respectively. Relative cell size was determined based on the median value of forward scatter (FSC) and normalized to control CMs. A minimum of 50,000 cells per samples were recorded.

For quantification of the efficiency of adenoviral delivery, iPSC-CMs were infected with adenovirus and analyzed by BD FACSARIA system (BD Biosciences, CA) seven days post-infection. Gating and population analysis were performed using FlowJo software.

Mice

All animal work described in this manuscript has been approved and conducted under the oversight of the UT Southwestern Institutional Animal Care and Use Committee. In this study, male wildtype C57BL/6J and ΔEx44 DMD mice previously generated in the C57BL/6J background using the CRISPR-Cas9 system[14] were used. Animals were allocated to experimental groups based on genotype. No animals were excluded from analyses and only male animals were used in this study due to X-chromosomal inheritance of DMD. Mice were housed in a barrier facility with a 12-hour light/dark cycle and maintained on standard chow (2916 Teklad Global). AAV9 production and delivery were performed as previously described[14]. Briefly, DMD ΔEx44 mice at postnatal day (P) 4 were intraperitoneally injected with an ultrafine needle (31 gauge, BD Ultra Fine U-100 Insulin Syringes). In this study, mice were injected with 80 µl of AAV9 preparations with a dosage of 8×10^{13} vg/kg of AAV-Cas9, and a 1:1 or 1:5 ratio of AAV-gRNA, respectively. Both of these dosages have previously been shown to effectively restore dystrophin expression in the murine heart[14]. 18 to 22-month old mice were used for snRNA-sequencing experiments to ensure that a cardiac phenotype is apparent as it was shown that conventional, single-knockout DMD mice exhibit a mild and delayed cardiac phenotype[7]. The sequence of the gRNA used in our mouse studies was as follows: 5'-CTTACAGGAACTCCAGGA-3'. The intron 44/ exon 45 junction of the *DMD* gene shares large homologies between human and mouse species[14] and we were able to target the same site in both our human and mouse studies.

Histopathological analysis of heart tissues

Processing of heart tissues, and H&E and Picro Sirius Red (PSR) staining were done was previously described[14]. Briefly, heart tissues were cryoembedded in Tissue Freezing Medium (Triangle Bioscience) and snap frozen in liquid nitrogen. Tissue blocks were stored at −80°C until to sectioning and thereafter. Eight-micrometer transverse sections of the hearts were prepared using a Leica CM3050 cryostat and air dried prior to staining. For Picrosirius Red Staining (PSR), cryosections of the hearts were thawed to room temperature and postfixed in 10% neutral-buffered formalin. Sections were rinsed in tap water before sensitization in heated Bouin's fixative (90 min at 60°C; Polysciences, Warrington, PA). Following tap water rinse, nuclei were counterstained with heated Weigert's iron hematoxylin. Following another tap water rinse, sections were stained with 0.1% Sirius red solution prepared in saturated aqueous picric acid for 1 hour. Sections were destained to collagen specificity with two washes of 0.5% glacial acetic acid, dehydrated, cleared, and coverslips were applied with permanent synthetic mounting media.

Dystrophin immunohistochemistry was performed using MANDYS8 monoclonal antibody (Sigma-Aldrich). Cryostat sections were thawed and rehydrated/delipidated in 1% Triton/

phosphate-buffered saline, pH 7.4 (PBS). Following delipidation, sections were washed and incubated with mouse immunoglobulin G (IgG) blocking reagent (M.O.M. Kit, Vector Laboratories). Primary antibody was added at 1:1800 in M.O.M. protein concentrate/PBS.and incubated overnight at 4°C. Dystrophin protein was detected using Alexa 594-conjugated secondary antibody (Thermo Fisher). Nuclei were counterstained with DAPI.

Single nucleus (sn)RNA-sequencing

Cardiac Nuclei Isolation and snRNA-sequencing: Cardiac nuclei isolation was performed as previously described[38]. Briefly, hearts of 18- to 22-month-old WT, DMD, and cDMD mice were extracted and dissected in ice-cold PBS. A transverse cut along the midline of base-apex axis was made for each heart and ventricular heart tissue below the cut was collected. For WT and DMD samples, we pooled two hearts of the same group for nucleus isolation. Hearts of cDMD mice were processed separately for nucleus isolation and sequencing. Total cardiac nuclei were used to generate single nucleus RNA-seq libraries using Single Cell 3' Reagent Kits v3 (10xGenomics) according to the manufacturer's protocol. In this study, we sequenced 3,624 nuclei of WT hearts, 1,650 nuclei of DMD hearts and 3,174 nuclei of cDMD hearts in accordance with previously published literature[39-42]

snRNA-seq Data Analysis: The Cell Ranger Single-Cell Software Suit (https://support.10xgenomics.com/single-cell-geneexpression/software/pipelines/latest/what-is-cell-ranger) was used to perform sample demultiplexing, barcode processing and single-cell 3′ gene counting. The cDNA reads were aligned to the mm10/GRCm38 premRNA reference genome. Only confidently mapped reads with valid barcodes and unique molecular identifiers were used to generate the gene-barcode matrix. Further analyses, including heatmap generation, GO analysis, Uniform Manifold Approximation and Projection (UMAP) analysis, were performed using the Seurat R package[43]. For quantity filtering, we removed cells that had more than 4000 or fewer than 200 detected genes. We then normalized the data by the total expression, multiplied by a scale factor of 10,000 and log-transformed the result. IntegrateData

function implemented in Seurat V3 was used to correct batch effects between samples and to merge samples into one Seurat object. To visualize the data, we used UMAP to project cells in 2D space on the basis of the aligned canonical correlation analysis[44]. Aligned canonical correlation vectors (1:30) were used to identify clusters using a shared nearest neighborhood modularity optimization algorithm. Cell clusters were identified using the FindCluster function in Seurat with resolution 0.6. We removed clusters with high median mitochondrial transcripts (>30% of total transcript coming from mitochondrial genes) that represent contamination of cell debris. Identities of the remaining cluster were assigned based on their marker gene expression using FindAllarkers shown in Online Figure XIV, whereby a Log fold-change >0.25 was used as the cutoff for top differentially expressed genes. We computationally merged the two cDMD samples for differential gene analysis and calculation of cellular composition. Differential gene analyses were performed using the Wilcoxon rank sum test on the scaled data. Differentially expressed genes with p-value < 0.0001 in any of the comparisons were used for GO analyses. For the presentation of changes in gene expression between the groups and various cell types, we surveyed genes that have consistently been reported to be of high significance for cardiomyocyte and fibroblast function in normal cardiac biology and cardiomyopathy[41, 45-48].

Data and Statistical analysis

Data collection and analysis of experiments shown in Fig. 1F-H, Fig. 2B-F, Fig. 4D, Fig. 4F-H, Fig. 5B and Online Figures IVA, VB, IXC, IXE, XIIIB were performed in a blinded fashion. Representative traces and images were selected by identifying those that most

closely represented the quantified average (for representations of quantified data) or by identifying those that were most similar to the rest of the dataset (for representations of non-quantified data). All data were analyzed using Graphpad Prism software (Graphpad Software) and presented as means ± SEM from the number of cells indicated in the text and figure legends. Normality was tested by visually inspecting the quantile-quantile (Q-Q) plot and frequency distribution for each dataset, and by performing D'Agostino-Pearson test (significance level 0.05). Statistical analysis of normally distributed data was performed using an ordinary one-way ANOVA followed by a Tukey post hoc analysis for equal variances or Brown-Forsythe and Welch one-way ANOVA followed by Dunnett T3 or Games-Howell post hoc analysis for unequal variances. Statistical analysis on non-normally distributed data was performed using Kruskal-Wallis test followed by Dunn's test correction. Statistical significance was defined as $p < 0.05$. Statistical tests are detailed in Online table II.

Online Table I. Primer sequences

Primer	Forward primer	Reverse primer
DMD Ex42-Ex46	GCCCTATTAGAAGTGGAACAAC	GGTTCAAGTGGGATACTAGC
RPL13A	CCTGGAGGAGAAGAGGAAAGAGA	TTGAGGACCTCTGTGTATTTGTCAA
RYR2	CCTTGCCTGAGTGCAGTTG	TTGAGGTATCAACAGGTTGTGG
NPPA	GTACTGAAGATAACAGCCAG	GATGTGAGAAGTGTTGACAG

NPPB	TGGAAACGTCCGGGTTACAG	CTGATCCGGTCCATCTTCCT

Online Table II: Details on statistical tests.

Figure	Normal Distribution	Statistical Test
1F	Yes	One-way ANOVA followed by Tukey post hoc analysis
1G	Yes	One-way ANOVA followed by Tukey post hoc analysis
1H	Yes	One-way ANOVA followed by Tukey post hoc analysis
2B	Yes	One-way ANOVA followed by Tukey post hoc analysis
2C	Yes	One-way ANOVA followed by Tukey post hoc analysis
2D	No	Kruskal-Wallis test followed by Dunn's test correction
2E	Yes	One-way ANOVA followed by Tukey post hoc analysis
2F	Yes	One-way ANOVA followed by Tukey post hoc analysis
4H	Yes	One-way ANOVA followed by Tukey post hoc analysis
OF IVA	No	Kruskal-Wallis test followed by Dunn's test correction
OF VB	Yes	Two-way ANOVA
OF VC	Yes	One-way ANOVA followed by Tukey post hoc analysis
OF VIC Left	Yes	One-way ANOVA followed by Tukey post hoc analysis
OF VIC Right	Yes	One-way ANOVA followed by Tukey post hoc analysis
OF VIII Left	Yes	One-way ANOVA followed by Tukey post hoc analysis
OF VIII Right	Yes	One-way ANOVA followed by Tukey post hoc analysis
OF IXC	Yes	One-way ANOVA followed by Tukey post hoc analysis
OF IXE	Yes	One-way ANOVA followed by Tukey post hoc analysis

Online Table III. Number of input genes included in GO Term analysis.

DMD vs cDMD-RF (794 genes)

GO Term	# genes associated with GO Term	# differentially regulated genes overlapping GO Term
extracellular matrix organization	395	82
cardiovascular system development	786	81
tissue morphogenesis	638	64
response to mechanical stimulus	202	35
collagen fibril organization	54	18
muscle contraction	349	39

heart development	556	50
actin cytoskeleton organization	696	51
cardiac muscle tissue development	209	23
regulation of membrane potential	431	33
regulation of heart contraction	246	21

DMD vs cDMD-ES (495 genes)

GO Term	# genes associated with GO Term	# differentially regulated genes overlapping GO Term
extracellular matrix organization	395	47
tissue morphogenesis	638	44
cardiovascular system development	786	44
muscle contraction	349	27
collagen fibril organization	54	11
regulation of membrane potential	431	26
heart development	556	30
cardiac muscle tissue development	209	16
regulation of heart contraction	246	16
actin cytoskeleton organization	696	29
cardiac muscle cell differentiation	114	9

Online Table IV. List of genes implicated in DCM and differentially expressed between DMD CMs and cDMD CMs.

Downregulated in DMD	ABCF1	EYA4	NAT8L	RNF220
	ACTA2	FADS3	NCOR2	S100A4
	ACTC1	FAM107A	NECTIN1	S1PR3
	ACTN2	FAM227A	NKX2-5	SAMHD1
	AKR1B1	FBLIM1	NMT1	SCN5A
	AKT1S1	FICD	NPPA	SEMA6B
	ANKRD1	FKRP	NPPB	SGCB
	ASTE1	FLNB	NPR3	SHISA4
	C1R	FLNC	NUCB1	SLC9A3R1
	CACNA1H	FLT1	NUP62	SMARCA4
	CALCOCO2	FTH1	OAZ1	SMPD3

	CCT4	GADD45B	OPTN	SRL
	CCT7	GNA11	PDLIM7	STARD10
	CD37	GPR137	PHLDA1	STAT3
	CD99	HCN4	PID1	STK40
	CDK2AP2	HFE	PIM3	TBC1D10B
	CHMP4B	HOPX	PKDCC	TFRC
	CKM	HRH2	PLEKHM2	TGFB2
	CNN1	IGF1R	PLPP7	TINAGL1
	CYB5R3	ITPR1	PLXNA1	TMEM165
	DAB2IP	ITSN1	POLH	TRIP10
	DBN1	KEAP1	PPIB	TRNT1
	DCP2	KIF18B	PRDM16	TRPV3
	DES	KRCC1	PTBP1	VASN
	DMD	LAMP1	PTMS	VCL
	DSP	LMOD1	PTTG1IP	WDR1
	DTNA	LTO1	PYGM	ZBTB10
	DYNC1LI2	MAP2K2	RASD1	ZBTB11
	EIF5A	MBD2	RBPMS2	ZBTB7B
	EMP3	MPST	RCAN2	
	EPHA4	MYH6	RDH10	
	EPN1	MYL9	RHOD	
Upregulated in DMD	AASS	FAM20C	MZT2A	RXRA
	ANXA2	FHL2	P2RX5-TAX1BP3	SDHA
	APBB1	FXN	PARP8	SGPP2
	ARRDC3	HADHA	PDCD5	SH3RF2
	ATP6V1E2	HMOX2	PDZRN3	SIAH1
	CA3	IGSF10	PLEKHO1	SLC12A7
	CACNA1D	ILK	PLN	SLC25A4
	CADPS2	ITGB1BP2	PPP1R15A	SNRPC
	CALR	KCNIP2	PPP1R1A	SOD2
	CCDC144NL-AS1	LAMA2	PRXL2A	SQSTM1
	CD34	LDHD	PTDSS1	SYNE2
	CLPP	MAP1LC3B	PTN	TESC
	CRYAB	MAVS	QSOX1	TMEM182
	CSRP2	MNS1	RAD1	TNNC1
	EBP	MPDU1	RAPGEF1	ZSCAN30
	EIF4EBP1	MTIF3	RBM20	
	ENTPD6	MYLK3	ROBO4	

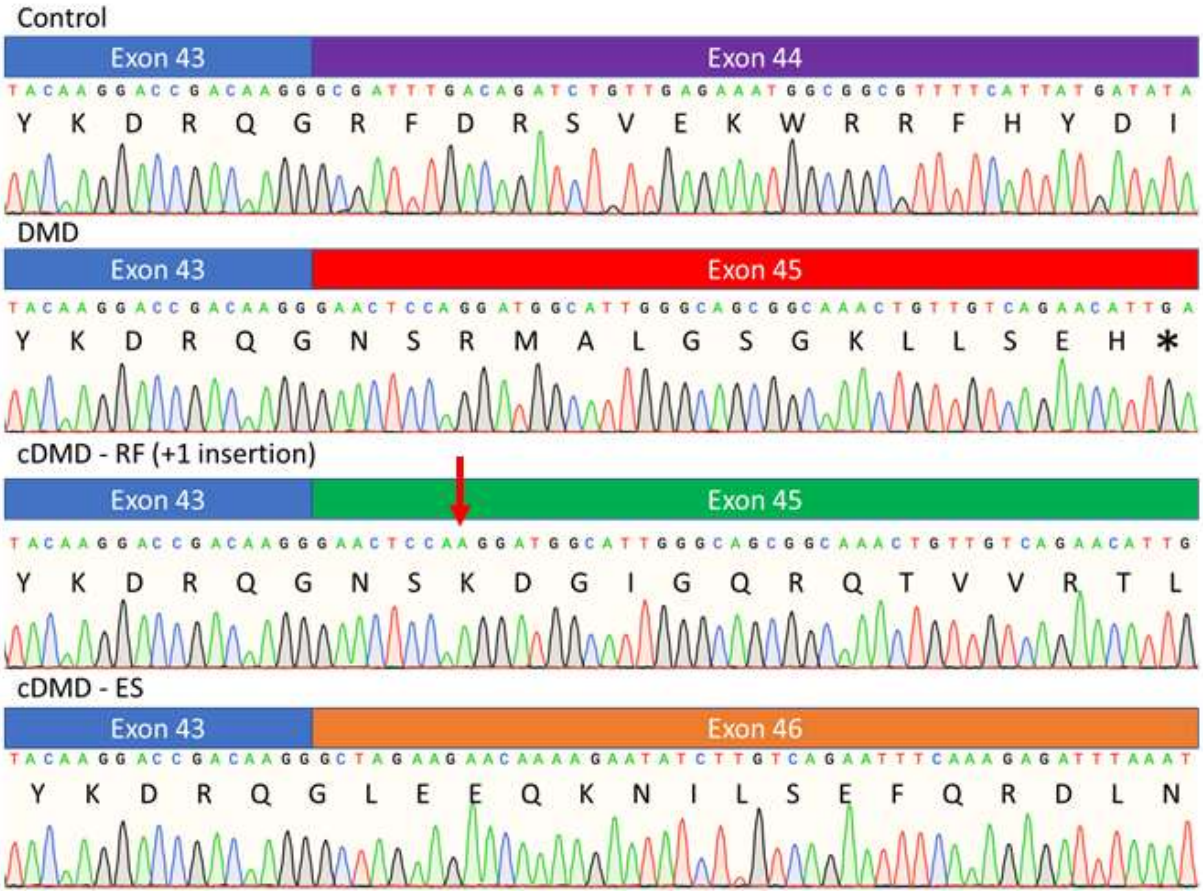

Online Figure I. Sanger sequencing of RT-PCR products using primers targeting exons 42 and 46 of DMD cDNA from control, DMD and cDMD-RF and cDMD-ES CMs. The asterisk denotes the presence of a stop codon in exon 45 of the DMD mRNA in DMD CMs. The red arrow points to the insertion of a single nucleotide to reframe exon 45.

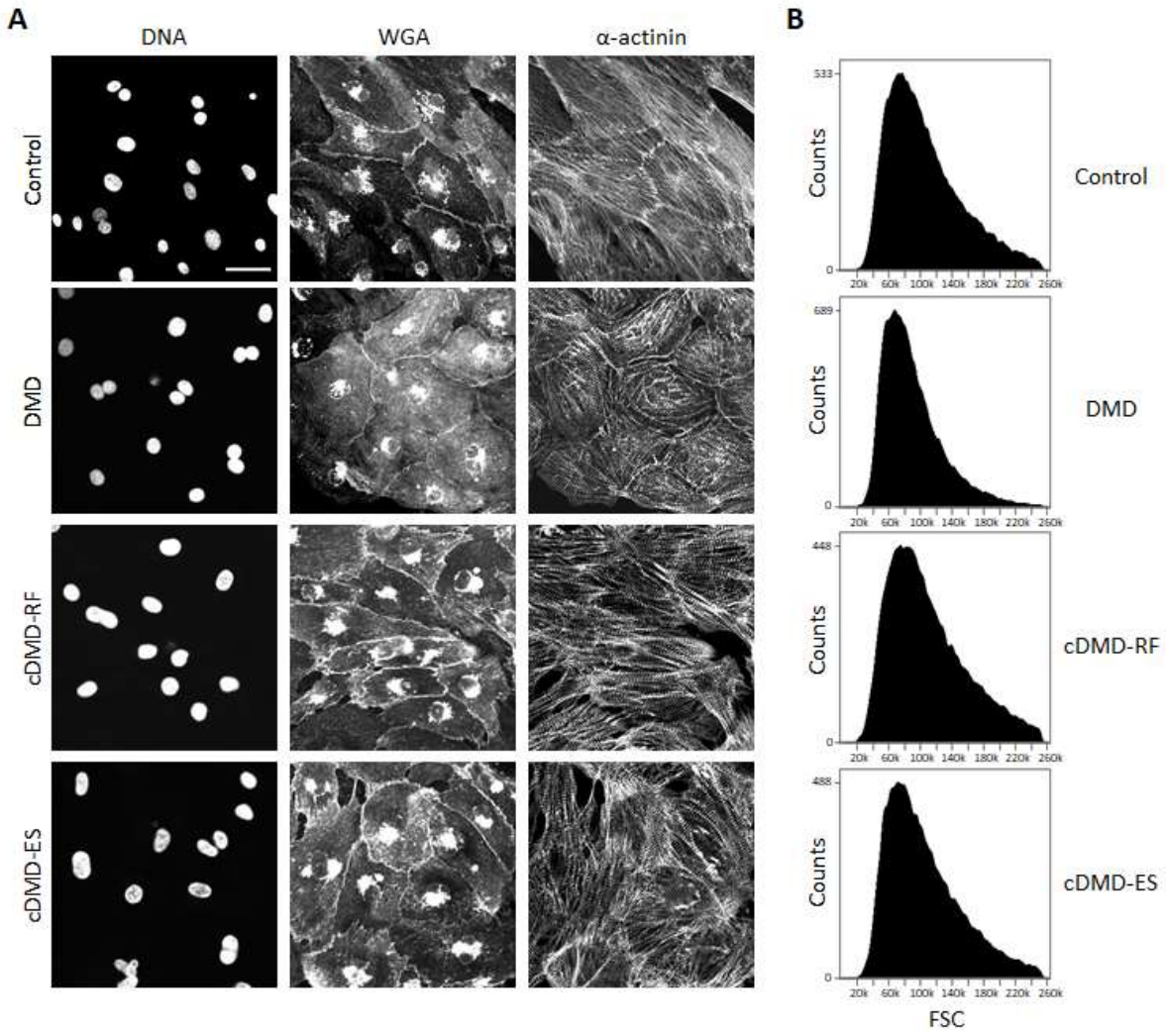

Online Figure II.

A) Representative immunofluorescence images of d35 control, DMD and cDMD CMs stained for wheat germ agglutinin and sarcomeric α-actinin. Scale bar 40μm.

B) Representative forward scatter histograms of d35 control, DMD and cDMD CMs.

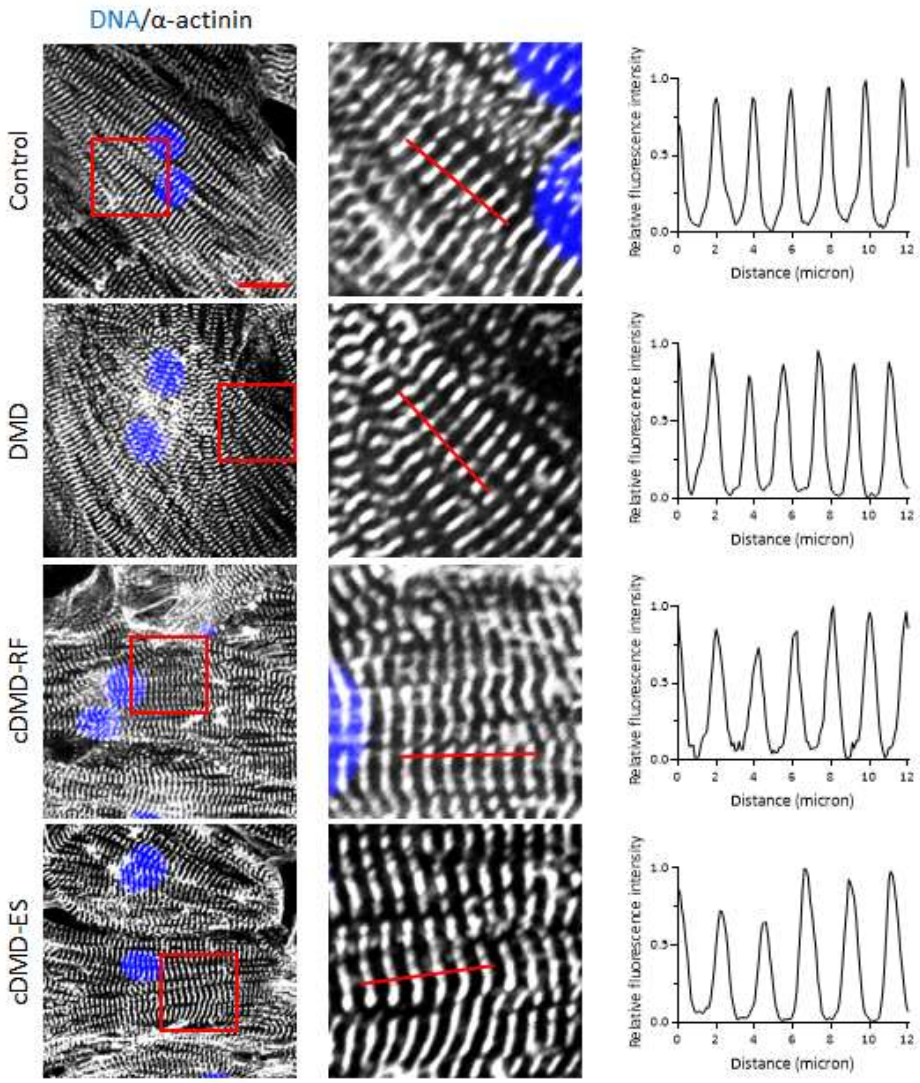

Online Figure III.

Quantification of sarcomere lengths. Intensity plot profiles across multiple Z-disks over a distance of 12μm are shown. Each graph starts from a peak. Scale bar 20μm.

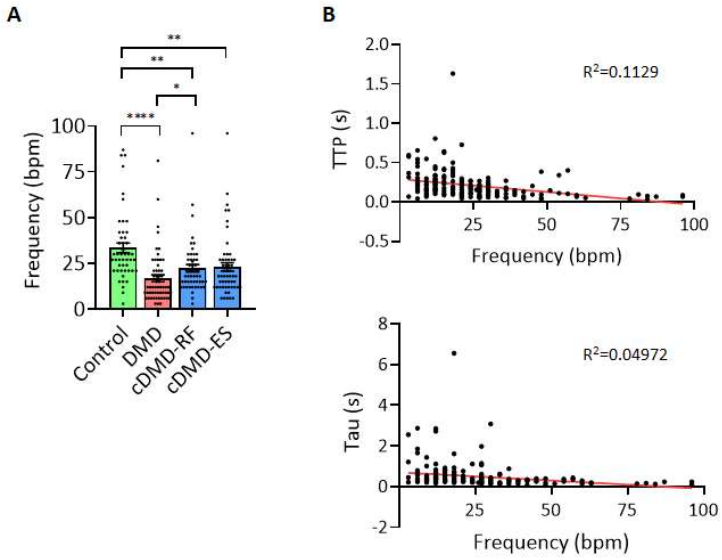

Online Figure IV.

A) Quantification of the contractile rate of iPSC-CMs during calcium handling measurements (Fig. 2). (n = 50 cells for control CMs, n = 56 cells for DMD CMs, n = 52 cells for cDMD-RF CMs, n = 54 cells for cDMD-ES CMs; quantification was performed across three independent batches of differentiation).

B) Summary of calcium handling parameters time to peak (TTP) and Tau (Fig. 2) as a function of the contractile rate of iPSC-CMs. Red lines represent linear regression curves.

Quantified data are shown as mean ± s.e.m. *p<0.05, **p<0.01 and ****p<0.0001.

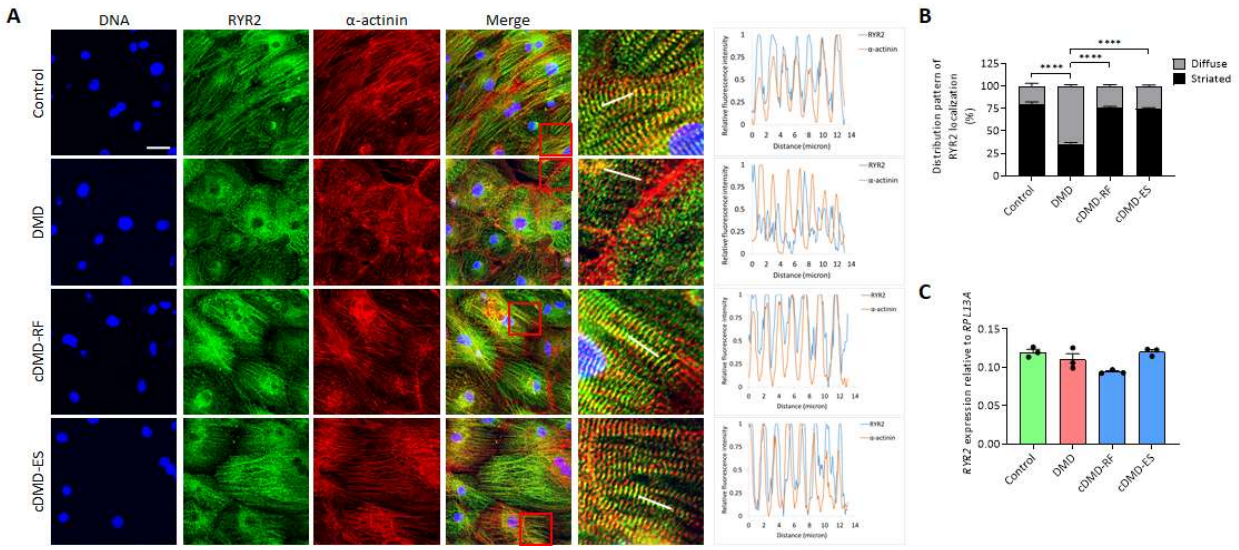

Online Figure V.

A) (Left) Representative immunofluorescence images of control, DMD and cDMD CMs stained for ryanodine receptor 2 (RYR2) and sarcomeric α-actinin. (Right) Intensity plot profiles across multiple Z-disks are shown. Scale bar 40μm.

B) Quantification of the localization pattern of RYR2 is shown. “Striated” is defined by an overlap of the fluorescence intensity signal of RYR2 with sarcomeric α-actinin, while “Diffuse” is defined by a random localization pattern of RYR2 independent of sarcomeric α-actinin (n = 373 cells for control CMs, n = 328 cells for DMD CMs, n = 317 cells for cDMD-RF CMs, n = 345 cells for cDMD-ES CMs; quantification was performed across three independent batches of differentiation).

C) Relative expression levels of *RYR2* in control, DMD and cDMD CMs based on quantitative PCR are shown (n = 3 samples per group across three independent batches of differentiation).

Experiments were performed at d35 post-differentiation. Quantified data are shown as mean ± s.e.m. ****p<0.0001.

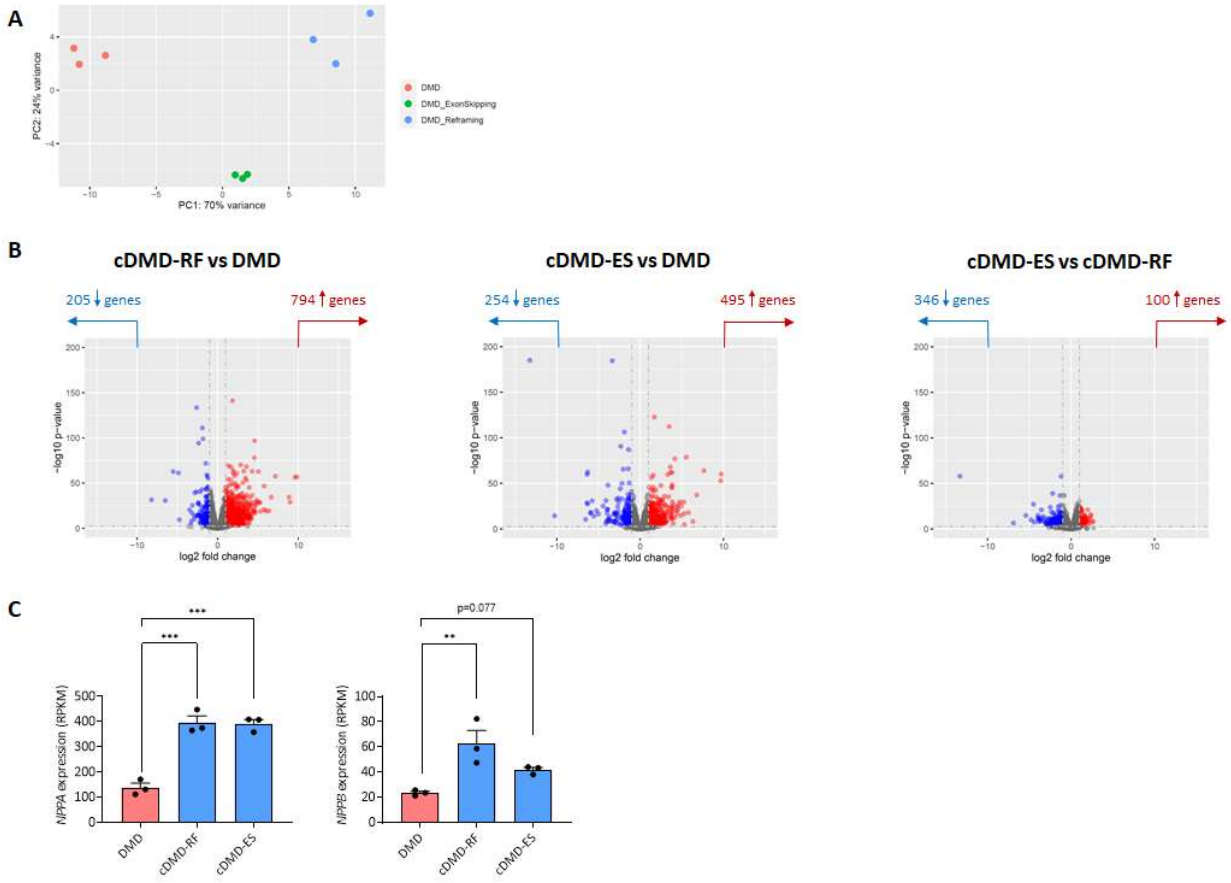

Online Figure VI.

A) Principal component analysis of RNA-sequencing performed on DMD and cDMD CMs.

B) Volcano plots of the significantly downregulated and upregulated genes in cDMD-RF versus DMD, cDMD-ES versus DMD and cDMD-ES versus cDMD-RF.

C) Relative expression levels of *NPPA* and *NPPB* in DMD and cDMD CMs based on RNA-sequencing data are shown (n = 3 samples per group across three independent batches of differentiation).

Quantified data are shown as mean ± s.e.m. **p<0.01 and ***p<0.001.

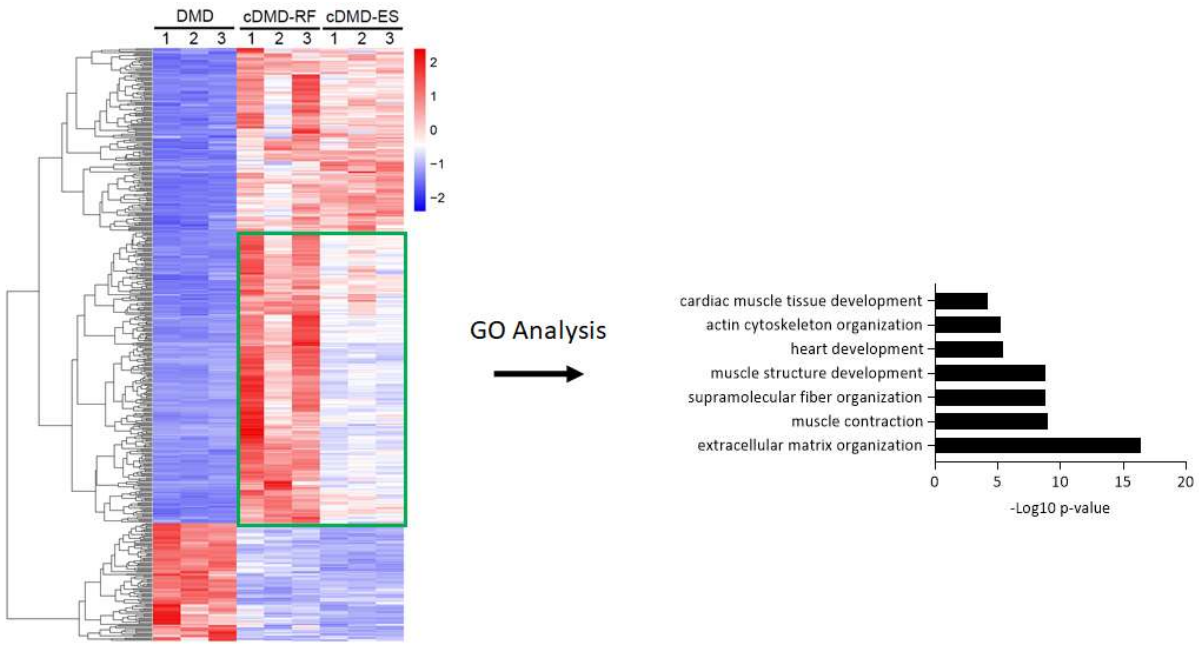

Online Figure VII.

Top GO terms associated with the differentially expressed genes marked with the green box in cDMD-RF versus cDMD-ES CMs.

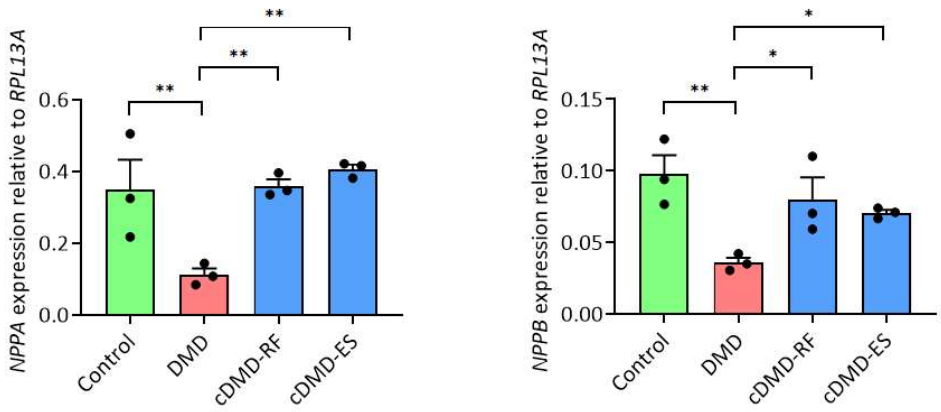

Online Figure VIII.

Relative expression levels of *NPPA* and *NPPB* in d50 control, DMD and cDMD CMs based on quantitative PCR are shown (n = 3 samples per group across three independent batches of differentiation).

Quantified data are shown as mean ± s.e.m. *p<0.05 and **p<0.01.

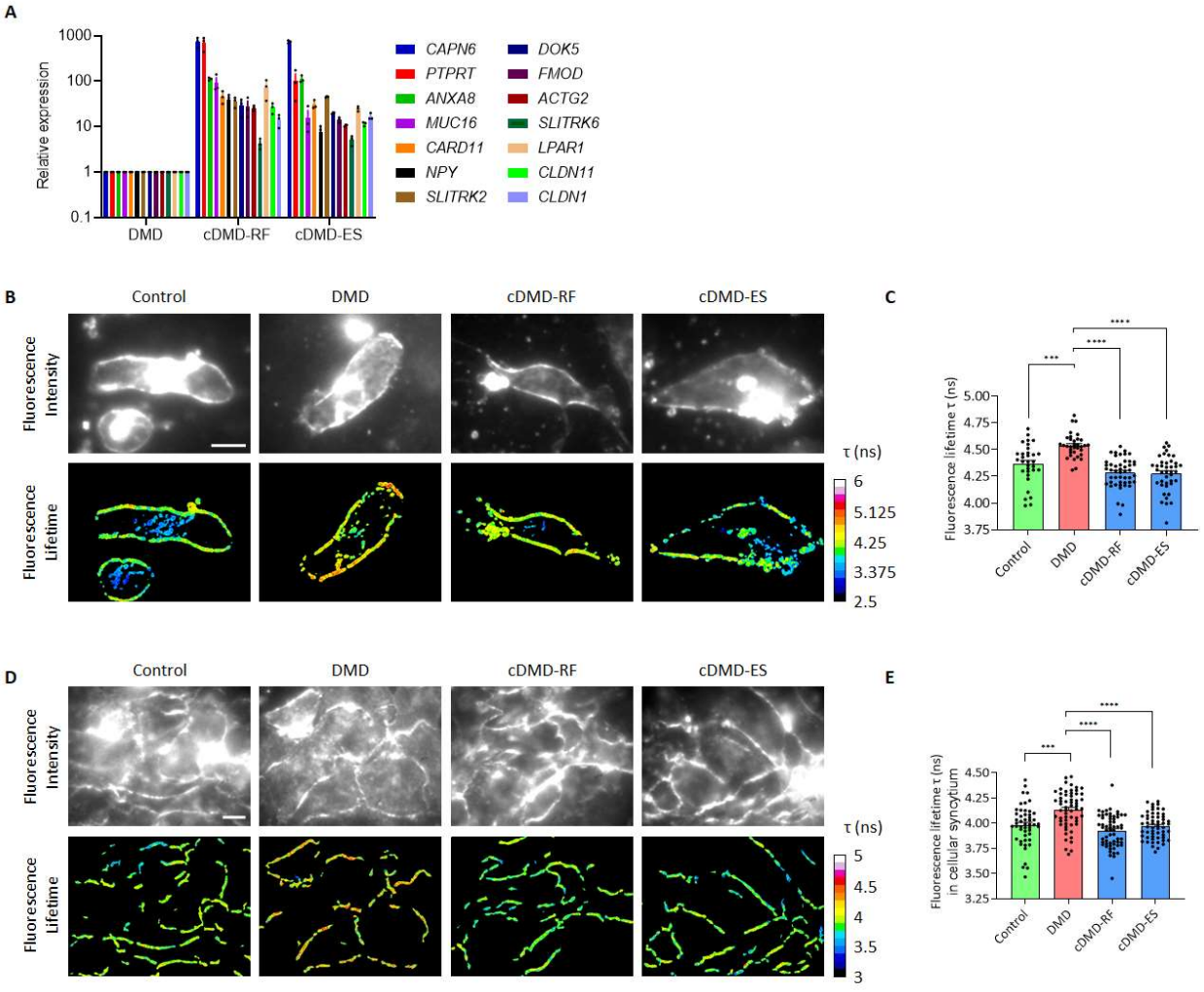

Online Figure IX.

A) Relative expression levels of genes involved in membrane biology and cytoskeletal organization in DMD and cDMD CMs based on RNA-sequencing data are shown (n = 3 samples per group across three independent batches of differentiation).

B) (Top) Representative fluorescence intensity images of single d50 control, DMD and cDMD CMs loaded with the membrane tension probe Flipper-TR and imaged by FLIM. (Bottom) Representative fluorescence lifetime images are computational analyses of the decay constant tau. Scale bar 20µm.

C) Quantification of the fluorescence lifetime of Flipper-TR in single d50 control, DMD and cDMD CMs (n = 32 cells for control CMs, n = 34 cells for DMD CMs, n = 47 cells for cDMD-RF CMs, n = 41 cells for cDMD-ES CMs; quantification was performed across three independent batches of differentiation).

D) (Top) Representative fluorescence intensity images of syncytial d50 control, DMD and cDMD CMs loaded with the membrane tension probe Flipper-TR and imaged by FLIM. (Bottom) Representative fluorescence lifetime images are computational analyses of the decay constant tau. Scale bar 25µm.

E) Quantification of the fluorescence lifetime of Flipper-TR in syncytial d50 control, DMD and cDMD CMs (n = 50 cells for control CMs, n = 59 cells for DMD CMs, n = 61 cells for cDMD-RF CMs, n = 56 cells for cDMD-ES CMs; quantification was performed across three independent batches of differentiation).

Quantified data are shown as mean ± s.e.m. ***$p<0.001$, ****$p<0.0001$.

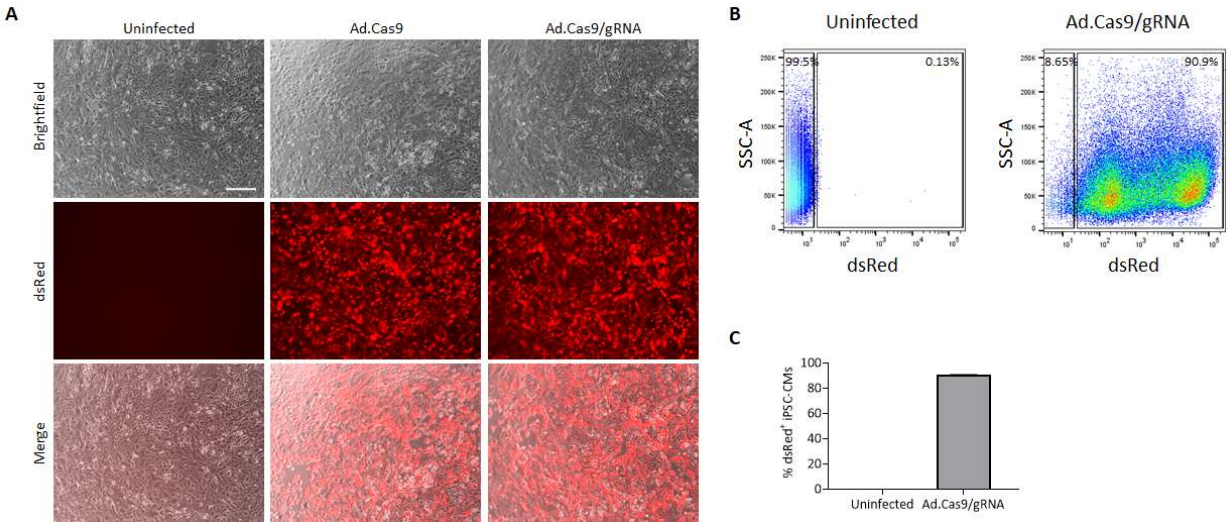

Online Figure X.

A) Representative images of uninfected CMs and CMs infected with Ad.Cas9 or Ad.Cas9/gRNA of the brightfield and dsRed channels. Scale bar 400µm.

B) FACS analysis of uninfected and infected iPSC-CMs.

C) Quantification of the percentage of CMs expressing dsRed after adenoviral infection based on FACS analysis (n = 3 samples per group across three independent batches of differentiation).

Images were acquired and analysis were performed 7 days post-infection. Quantified data are shown as mean ± s.e.m. ****p<0.0001.

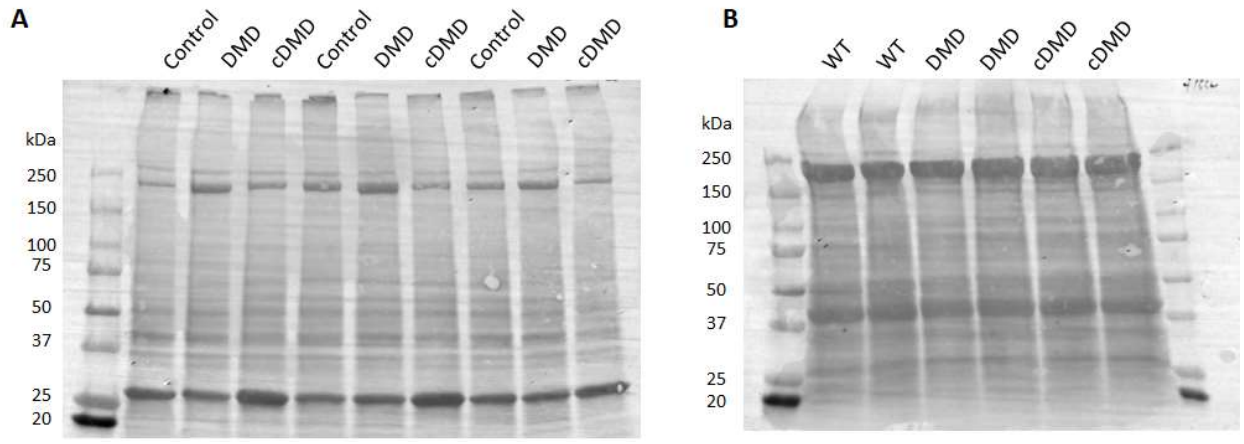

Online Figure XI.

A) Total protein loading control for the quantification of dystrophin correction in iPSC-CMs. Related to Fig. 4D.

B) Total protein loading control for the quantification of dystrophin correction in mice. Related to Fig. 5B.

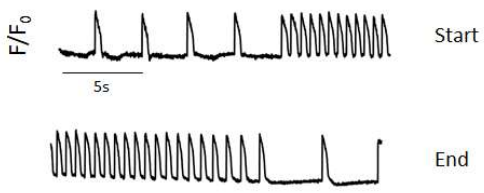

Online Figure XII.

Representative membrane potential traces of DMD CMs loaded with the voltage-sensitive probe FluoVolt entering (top) or quitting (bottom) a tachyarrhythmic episode.

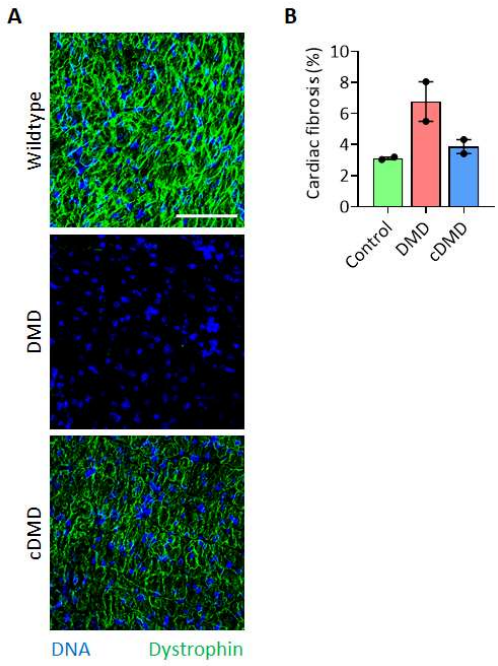

Online Figure XIII.

A) Representative immunofluorescence images of sections of hearts from wildtype (WT), DMD and corrected DMD mice. Scale bar 100µm.

B) Quantification of cardiac fibrosis in sections of hearts from wildtype (WT), DMD and corrected DMD mice stained with Picro Sirius Red as shown in Fig. 5C (n = 2 samples per group).

Quantified data are shown as mean ± s.e.m.

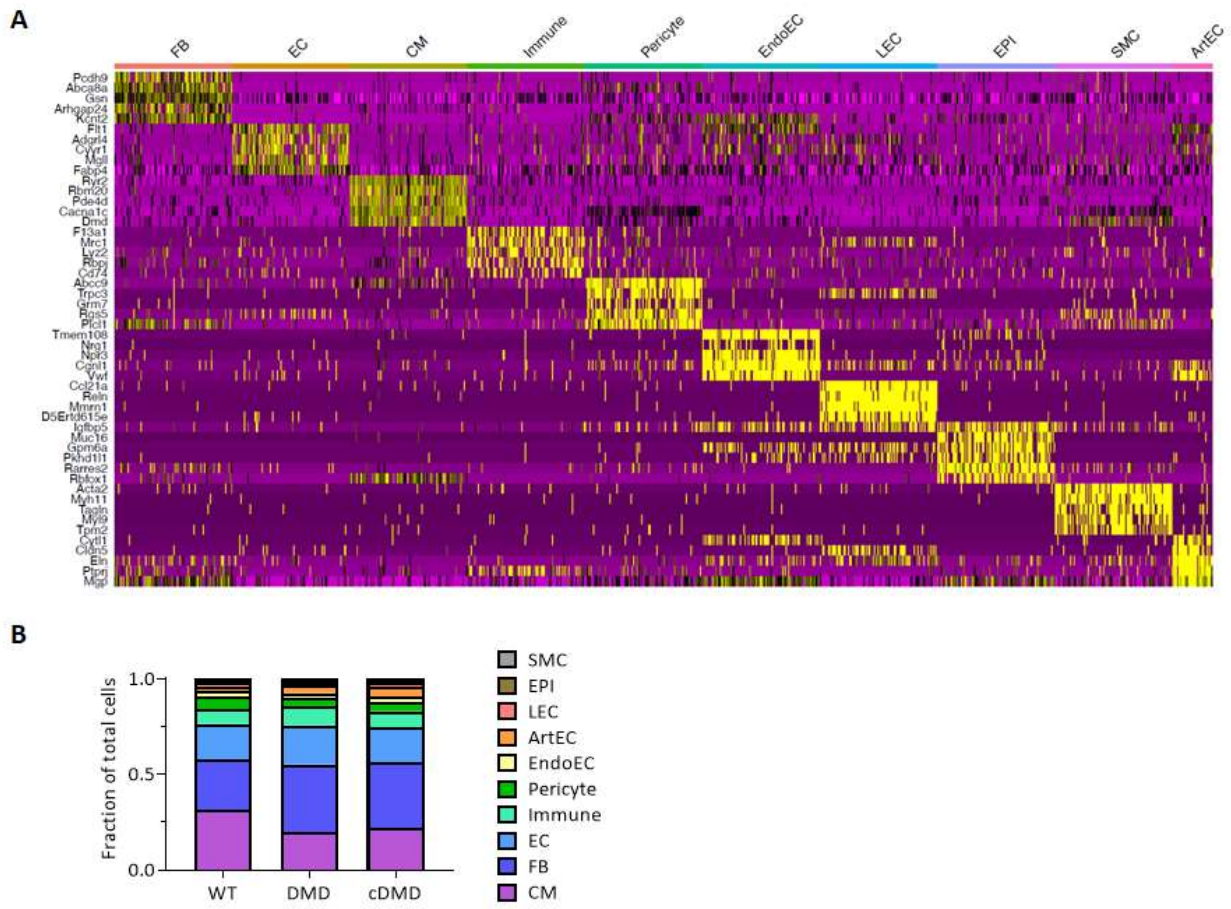

Online Figure XIV.

A) Gene signatures of cardiac cell populations. Expression levels of top five markers for each cluster are shown.

B) Fraction of cardiac cell populations in each WT, DMD and cDMD samples.

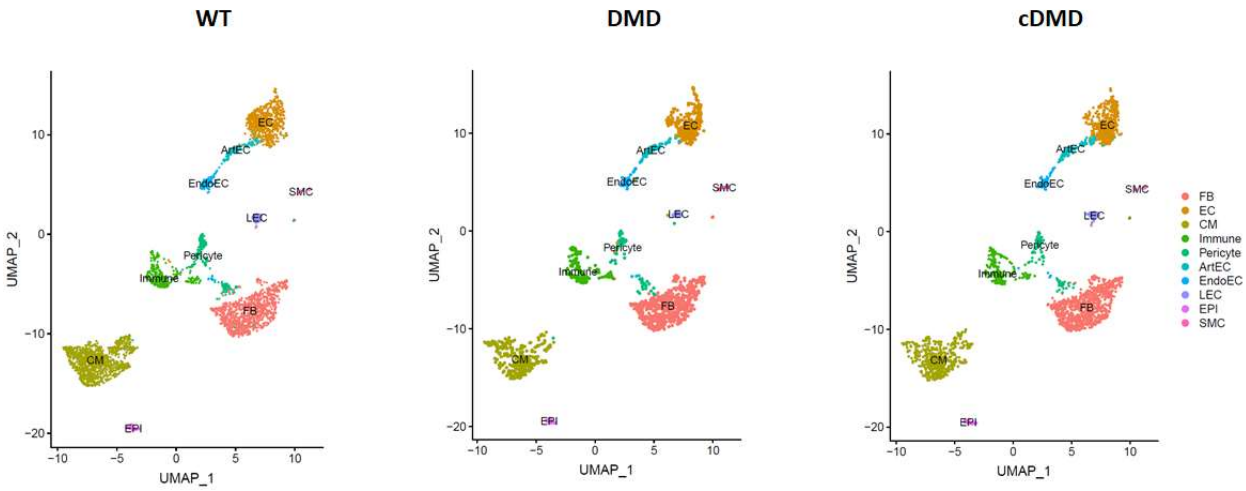

Online Figure XV.

UMAP visualization of all of the nuclei from WT, DMD and cDMD hearts colored by cluster identity.

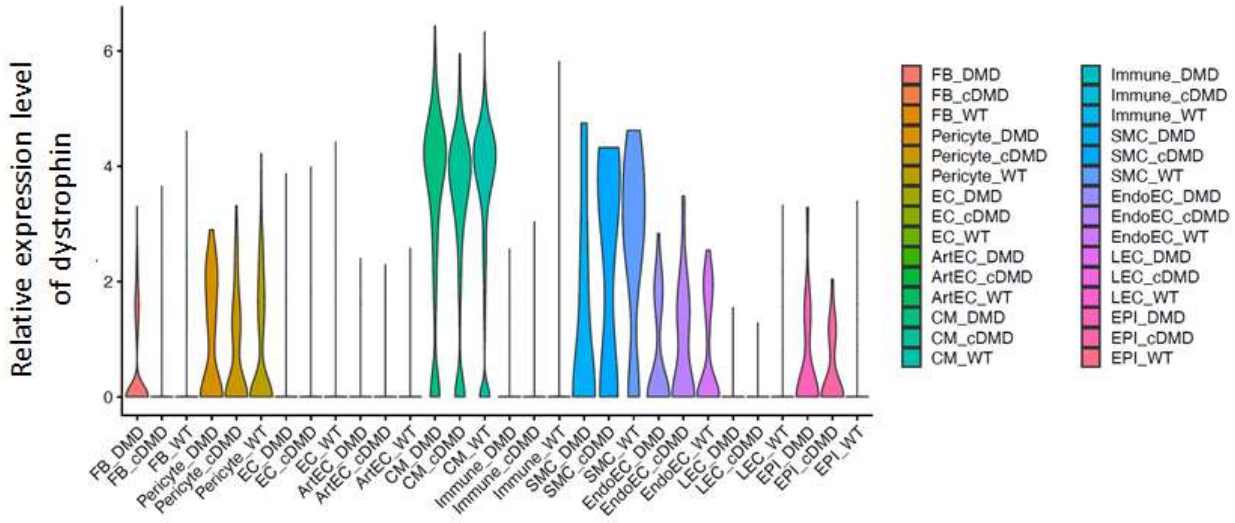

Online Figure XVI.

Violin plot showing the expression of dystrophin for each cluster of nuclei in each wildtype (WT), DMD and corrected DMD (cDMD) hearts.